Protein Folding

DOI: 10.1002/ange.201308512

An Off-Pathway Folding Intermediate of an Acyl Carrier Protein Domain Coexists with the Folded and Unfolded States under Native Conditions**

*Jackwee Lim, Tianshu Xiao, Jingsong Fan, and Daiwen Yang**

Abstract: *A protein can exist in multiple states under native conditions and those states with low populations are often critical to biological function and self-assembly. To investigate the role of the minor states of an acyl carrier protein, NMR techniques were applied to determine the number of minor states and characterize their structures and kinetics. The acyl carrier protein from Micromonospora echinospora was found to exist in one major folded state (95.2 %), one unfolded state (4.1 %), and one intermediate state (0.7 %) under native conditions. The three states are in dynamic equilibrium and the intermediate state very likely adopts a native-like structure and is an off-pathway folding product. The intermediate state may mediate the formation of oligomers in vitro and play an important role in the recognition of partner enzymes in vivo.*

According to the protein-folding energy landscape,[1] a protein exists in a conformational equilibrium between multiple states, the populations of which follow a Boltzmann distribution.[2,3] Owing to their low populations and short lifetimes, it is difficult to detect and characterize minor states under native conditions,[3] although they are known to play critical roles in the regulation of biological function[4,5] and in the formation of protein aggregates, which is associated with misfolding diseases and silk fibers.[6] In favorable cases, the presence of the minor states can be demonstrated by spectroscopic techniques such as nuclear magnetic resonance (NMR), circular dichroism (CD), and fluorescence spectroscopy.[3,7] With the recent developments in NMR spectroscopy, 3D structure determination of a minor state is now feasible when its population is larger than 0.5 % and its lifetime is longer than 1 ms.[8] Even with such structural information, it is still difficult to differentiate minor on-pathway species from off-pathway folding species that may cause fibril formation.[9,10] Fortunately, by obtaining kinetic parameters, one may tell whether the minor state is an on-pathway or off-pathway species. Herein, we report the identification of an off-pathway intermediate state of the acyl carrier protein domain from *Micromonospora echinospora spp. calichensis* (*me*ACP) based on chemical exchange saturation transfer (CEST) data.

*me*ACP is a type I ACP that catalyzes the transfer of acyl intermediates between the domains of the type I fatty acid synthase (FAS) and polyketide synthase (PKS) systems. Unlike type I ACP, which is part of a large FAS/PKS polypeptide system, type II ACP is a small free-standing protein. Nonetheless, in both synthase systems, ACP is essential for the transfer of the acyl intermediates between different catalytic sites.[11] *me*ACP consists of three helices connected by two long loops, which are nearly as rigid as the helices on nanosecond–picosecond timescales.[12,13] Through relaxation dispersion (RD) experiments, we have recently shown that *me*ACP exists in more than one state in solution under native conditions.[13] On the basis of the ^{15}N chemical shifts extracted from fitting the RD data to a global two-state model, the minor state corresponds to a mainly disordered conformation. We have also demonstrated that the disordered conformation can be eliminated by stabilizing the folded major state through the introduction of a disulfide linkage between helices 1 and 3.[13] In order to investigate whether *me*ACP exists in more than two states in solution, we performed the CEST experiments described herein.

If a minor state undergoes conformational exchange with a major state, saturation of a nuclear spin in the minor state will cause signal reduction of this spin in the major state. Scanning the frequency of the weak radiofrequency (rf) field that is applied for saturation transfer, one can determine the number of invisible minor states, their resonant frequencies, and the kinetic parameters for a given nuclear spin provided that the exchange between the visible major and invisible minor states is relatively slow.[14,15] Through CEST experiments, we found that while most of the residues in *me*ACP exist in one major state (corresponding to the big dip) and one minor state (corresponding to the small dip; Figure 1), several residues exist in one major state and two minor states (Figure 2). Notably, 34 residues showed two obvious dips that are separated by more than 160 Hz (Figure 1 a, b) and their CEST data could be fitted to a global two-state exchange model ($N \rightleftharpoons^{k_{ex}} U$, where N and U represent the major and minor states, respectively, and k_{ex} is the total exchange rate). The resultant k_{ex} and population of the minor state (P_u) values were $(218 \pm 6)\ s^{-1}$ and $(4.7 \pm 0.1)\,\%$, respectively. In addition, 26 residues displayed either two dips separated by less than 160 Hz or just one asymmetric dip (Figure 1 c) and their ^{15}N chemical shifts in the minor state (δ_U) were calculated by fitting the CEST data to a global two-state exchange model with fixed kinetic parameters ($k_{ex} = 218\ s^{-1}$ and $P_u = 4.7\,\%$) obtained from the global fitting. According to the resultant δ_U

[*] Dr. J. Lim, T. Xiao, Dr. J. Fan, Prof. D. Yang
Department of Biological Sciences
National University of Singapore
14 Science Drive 4, Singapore 117543 (Singapore)
E-mail: dbsydw@nus.edu.sg

[**] This research was supported by a grant from Singapore Ministry of Education (Academic Research Fund Tier 3, MOE2012-T3-1-008).

Supporting information for this article is available on the WWW under http://dx.doi.org/10.1002/anie.201308512.

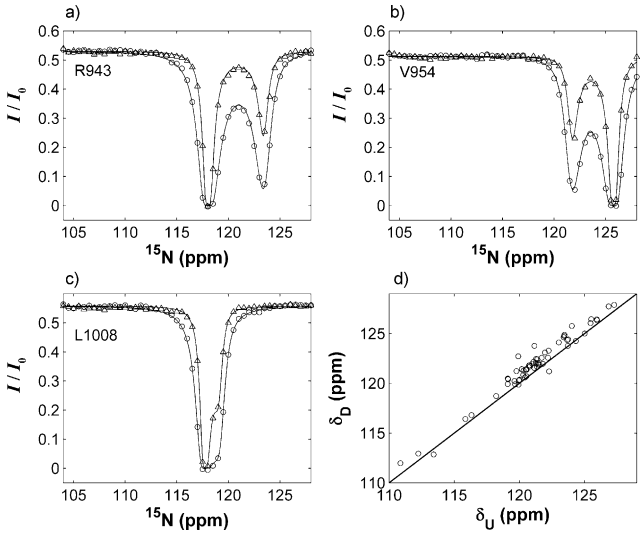

Figure 1. Representative CEST profiles with two dips that could be fitted to a global two-state model (a–c) and a comparison of the ^{15}N chemical shifts in the unfolded U state (δ_U) derived from the CEST data and in the denatured state (δ_D) in the presence of 4 M urea (d). The data points obtained at weak rf fields of 15 and 30 Hz are shown as triangles and circles, respectively. The solid curves in parts a–c are the best fits with a two-state model.

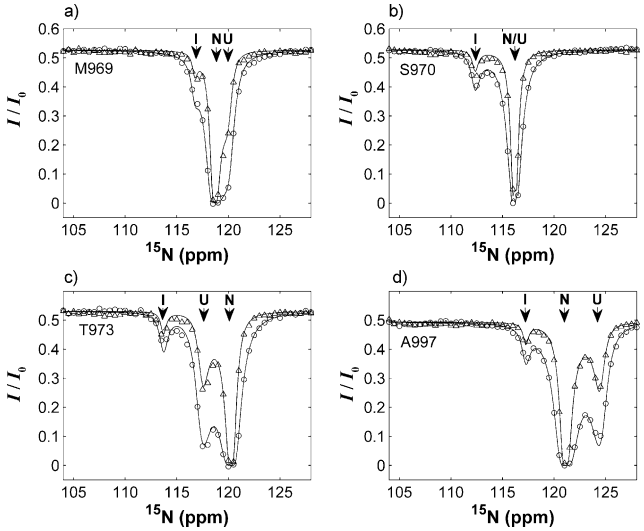

Figure 2. Representative CEST profiles with three obvious dips (a, c, and d) or two dips that could not be fitted to the global two-state model (b). The data points obtained at weak rf fields of 15 and 30 Hz are shown as triangles and circles, respectively. The solid curves are the best fits with model 1.

values and experimental ^{15}N shifts of the denatured state in 4 M urea (δ_D; Figure 1 d, Table S1 in the Supporting Information), the minor state should be mainly unfolded, a result consistent with the conclusion drawn from the RD data, and is thus denoted as U. Hence the conformational exchange process probed by the CEST experiment is very likely the folding–unfolding equilibrium of *me*ACP. The k_{ex} and P_u values obtained from the CEST data are different from those calculated from the RD data (301 s^{-1} and 3.4 %), but the unfolding rates ($k_{ex} \times P_u$) and δ_U values calculated from the CEST and RD data are almost identical (Figure S1 in the Supporting Information). This is because the RD profile is more sensitive to the product of k_{ex} and P_u than to the individual values in a regime of relatively slow exchange on the NMR timescale.[14] In fact, the RD data could also be fitted to the kinetic parameters derived from the CEST data but with a slightly larger χ^2 value (1126 vs. 857).

For the residues displaying three obvious dips (M969, T973, V978, T994, and A997; Figure 2 and Figure S2), their CEST data could be fitted to the following three-state model (model 1):

$$\mathrm{I} \underset{}{\overset{k_{2ex}}{\rightleftharpoons}} \mathrm{N} \underset{}{\overset{k_{1ex}}{\rightleftharpoons}} \mathrm{U} \quad (1)$$

The kinetic parameters obtained were $P_u = (4.1 \pm 0.1)\,\%$, $P_I = (0.7 \pm 0.1)\,\%$, $k_{1ex} = (248 \pm 12)\ s^{-1}$, and $k_{2ex} = (111 \pm 17)\ s^{-1}$ where P_u (P_I) is the population of state U (I) and k_{1ex} (k_{2ex}) is the total exchange rate for the equilibrium between states N and U (N and I). According to the ^{15}N chemical shifts of the two minor states (Table S2), one minor state should adopt a mainly unfolded conformation (U), whereas the other minor state is definitely different from both the unfolded and native conformations and is thus named as an intermediate state (I). The population of state N (95.2 %) and the unfolding rate from state N to state U ($P_u \times k_{1ex} = 10.17\ s^{-1}$) are consistent with the values derived from the residues showing only two conformations (95.3 % and 10.25 s^{-1}), thus suggesting that the entire protein is in a dynamic unfolding–folding equilibrium. Besides this global process, several residues in state N also undergo conformational exchanges involving both minor states. Two scenarios can be envisaged. In the first scenario, state I resembles state N in overall structure, that is, most of the ^{15}N spins have similar chemical shifts in the I and N states and display only two CEST dips like those shown in Figure 1; one corresponding to state U and the other to the sum of states N and I. In the second scenario, state I resembles state U in overall structure, that is, most residues in state I undergo folding–unfolding with state N and their I-state dips overlap with their U-state dips. The two scenarios cannot be differentiated by our CEST and RD data.

The data could also be fitted to another three-state model (model 2):

$$\mathrm{N} \underset{}{\overset{k_{2ex}}{\rightleftharpoons}} \mathrm{U} \underset{}{\overset{k_{1ex}}{\rightleftharpoons}} \mathrm{I} \quad (2)$$

The resultant kinetic parameters were $P_u = (4.1 \pm 0.1)\,\%$, $P_I = (0.7 \pm 0.1)\,\%$, $k_{1ex} = (234 \pm 10)\ s^{-1}$, and $k_{2ex} = (137 \pm 21)\ s^{-1}$, which are similar to the values obtained from model 1. In this model, state I can resemble either state U or state N in overall structure. No matter which model applies to *me*ACP, the I state is an off-pathway product.

The on-pathway folding model (model 3) was also used to fit the experimental data.

$$\mathrm{N} \underset{}{\overset{k_{2ex}}{\rightleftharpoons}} \mathrm{I} \underset{}{\overset{k_{1ex}}{\rightleftharpoons}} \mathrm{U} \quad (3)$$

The χ^2 values for model 3 (e.g., 3937 for T973) are much larger than those for models 1 (265 for T973) and 2 (192 for

T973) when M969, T973, V978, T994, and A997 were fitted either individually or simultaneously. In fact, many of the experimental data points are quite far away from the best fits for model 3 (Figure S3). Therefore, model 3 cannot be used to describe the dynamic process of *me*ACP.

Although the CEST profiles of S970, L977, E980, and A981 display only one obvious minor dip (Figure 2b and Figure S2), they could not be fitted to the global two-state exchange model. Instead, they were fitted to models 1 and 2. The chemical shifts of these residues in state N are similar to those in state U (convoluted as one major dip), but very different from those in state I (Table S2), thus explaining the observation of only one minor dip (corresponding to state I). According to models 1 and 2, the contribution of state I to the ^{15}N relaxation dispersion is less than 1 s^{-1}. Therefore, the RD data for all of the residues displaying three states could still be fitted reasonably well to a two-state model.

Except for T994 and A997, which are in the long loop between helices 2 and 3 in the native structure, the other residues that show three states (M969, S970, T973, L977, V978, E980, and A981) are located predominantly in the N-terminal region of helix 2, also known as the "recognition helix" for universal enzyme interaction in carrier proteins.[11] The N state does not contain any large and contiguous hydrophobic patches and its surface is quite hydrophilic (Figure 3), a fact consistent with the high water solubility of *me*ACP (> 1.5 mM). If state I differs from state N only in the local structure of the N-terminal region of helix 2, state I may have more solvent-exposed hydrophobic patches formed by the residues in the helix-2 region, which are completely buried in state N (Figure 3). This suggests that state I is likely prone to form oligomers.

Based on the ^{15}N relaxation times T_1 and T_2, the overall tumbling time of *me*ACP was found to be 7.5 ns, a value significantly larger than that for the A938C/E1009C mutant, which has a disulfide linkage between helices 1 and 3 (6.8 ns). The longer overall tumbling time indicates the presence of oligomers in the wild type protein and that the oligomers are in a dynamic equilibrium with the observed monomer. To confirm the existence of oligomers, we also performed sedimentation velocity (SV) experiments on both wild type and mutant *me*ACP through analytical ultracentrifugation (AUC). The apparent molecular weight (MW) of *me*ACP [(14.5 ± 1.8) kDa at 2.5 mg mL^{-1} and (15.6 ± 1.3) kDa at 7.5 mg mL^{-1}] was significantly larger than that of the mutant [(11.3 ± 1.2) kDa at 2.5 mg mL^{-1} and (11.0 ± 1.3) kDa at 7.5 mg mL^{-1}; Figure S4], thus demonstrating that oligomers exist for wild type *me*ACP. Since the oligomers and the monomer are in rapid reversible equilibrium on the timescale of sedimentation (minute), the SV peaks corresponding to the oligomers could not be resolved. Given that the apparent MW of the mutant is almost the same as its MW (11.2 kDa), the mutant should not form oligomers under our experimental conditions. Furthermore, the structures of the N state and the mutant are nearly identical,[13] so the N state should not form oligomers either. To examine whether it is the U state that is prone to forming oligomers, we next carried out CD and 1D ^{1}H NMR experiments. The CD profile at 25 °C is identical to that for the same sample heated to 60 °C and then slowly cooled down to 25 °C (Figure S5), thus indicating that the unfolded species does not aggregate. The ^{1}H NMR spectrum at 25 °C is also the same in terms of intensity and linewidth as that for the same sample heated to 60 °C and then cooled down to 25 °C (Figure S6A). At 60 °C, the protein is completely unfolded (Figure S6B) and the sharp peaks in the aromatic region ($\delta = 6.5$–7.5 ppm) also indicate that the unfolded protein does not form large oligomers. Taken together, the oligomers should result from the presence of state I rather than states N or U and state I likely resembles state N. This agrees with recent results from other groups, which support the idea that the aggregation of globular proteins occurs through native-like intermediates with local unfolding.[10,16]

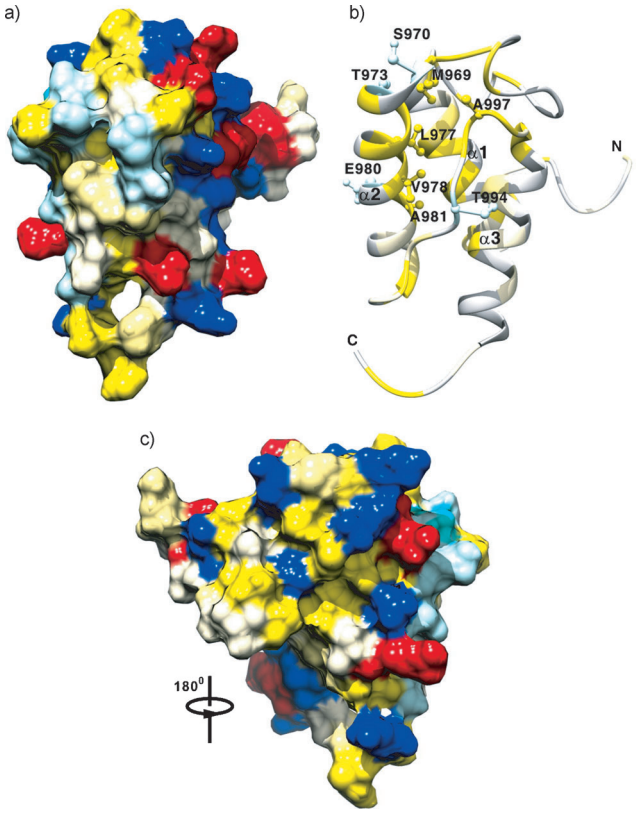

Figure 3. Surface plots (a, c) and a ribbon diaram (b) of *me*ACP. In the surface plots, hydrophobic residues are colored by a scale based on normalized hydrophobicity values: Phe (1.0) yellow, Val (0.57) pale yellow, and Gly (0.0) white. Positively charged, negatively charged, and polar residues are colored in blue, red, and pale blue, respectively. In the ribbon diagram, the side chains of the residues that display three conformational states are shown, and the hydrophobic residues are indicated in yellow.

Based on the available crystal structure of type II ACP in complex with its activator AcpS from *Bacillus subtilis*, the three ACP molecules are spatially separated in the trimeric assembly of AcpS[17] and hence *me*ACP likely exists as a folded monomer in the active state in vivo. More importantly, the ACP–AcpS structure clearly shows that the ACP–AcpS interaction involves the recognition helix 2 (numbered helix 3 in *Bacillus subtilis* ACP) and mutagenesis has also shown that helix 2 is indeed vital for the function of ACP.[18]

Because the interaction is presumably weak or transient in many synthase systems, it is not well understood how a single ACP unit can recognize different enzymes for catalysis. Perhaps, the presence of intermediates or subtle restructuring of helix 2 as observed here is important for ACP to successfully recognize a number of partner enzymes or catalytic domains at different stages during biosynthesis.

In summary, we have demonstrated that *me*ACP exists in three states (folded, unfolded, and intermediate), which undergo conformational exchange on the timescale of approximately 4–10 ms. The intermediate state, which involves recognition helix 2, was shown to be an off-pathway rather than on-pathway folding product and it may mediate the formation of oligomers in vitro and play an important role in the recognition of partner enzymes in vivo.

Received: September 30, 2013
Revised: December 12, 2013
Published online: January 27, 2014

Keywords: acyl carrier protein · folding intermediates · protein dynamics · protein folding · protein structure

[1] P. G. Wolynes, J. N. Onuchic, D. Thirumalai, *Science* **1995**, *267*, 1619 – 1620.
[2] K. Henzler-Wildman, D. Kern, *Nature* **2007**, *450*, 964 – 972.
[3] D. J. Brockwell, S. E. Radford, *Curr. Opin. Struct. Biol.* **2007**, *17*, 30 – 37.
[4] D. Kern, B. F. Volkman, P. Luginbühl, M. J. Nohaile, S. Kustu, D. E. Wemmer, *Nature* **1999**, *402*, 894 – 898.
[5] A. Matouschek, *Curr. Opin. Struct. Biol.* **2003**, *13*, 98 – 109.
[6] F. Chiti, C. M. Dobson, *Annu. Rev. Biochem.* **2006**, *75*, 333 – 366.
[7] J. L. Neira, *Arch. Biochem. Biophys.* **2013**, *531*, 90 – 99.
[8] D. M. Korzhnev, L. E. Kay, *Acc. Chem. Res.* **2008**, *41*, 442 – 451.
[9] D. M. Korzhnev, T. L. Religa, W. Banachewicz, A. R. Fersht, L. E. Kay, *Science* **2010**, *329*, 1312 – 1316.
[10] P. Neudecker, P. Robustelli, A. Cavalli, P. Walsh, P. Lundström, A. Zarrine-Afsar, S. Sharpe, M. Vendruscolo, L. E. Kay, *Science* **2012**, *336*, 362 – 366.
[11] D. M. Byers, H. Gong, *Biochem. Cell Biol.* **2007**, *85*, 649 – 662.
[12] J. Lim, R. Kong, E. Murugan, C. L. Ho, Z. X. Liang, D. Yang, *PLoS One* **2011**, *6*, e20549.
[13] J. Lim, H. Sun, J. S. Fan, I. F. Hameed, J. Lescar, Z. X. Liang, D. Yang, *Biophys. J.* **2012**, *103*, 1037 – 1044.
[14] P. Vallurupalli, G. Bouvignies, L. E. Kay, *J. Am. Chem. Soc.* **2012**, *134*, 8148 – 8161.
[15] N. L. Fawzi, J. Ying, D. A. Torchia, G. M. Clore, *J. Am. Chem. Soc.* **2010**, *132*, 9948 – 9951.
[16] F. Chiti, C. M. Dobson, *Nat. Chem. Biol.* **2009**, *5*, 15 – 22.
[17] K. D. Parris, L. Lin, A. Tam, R. Mathew, J. Hixon, M. Stahl, C. C. Fritz, J. Seehra, W. S. Somers, *Structure* **2000**, *8*, 883 – 895.
[18] H. Gong, A. Murphy, C. R. McMaster, D. M. Byers, *J. Biol. Chem.* **2007**, *282*, 4494 – 4503.

